

FIG. 2. Proton electric FF data in the spacelike ($t < 0$) region from MAMI [16].

Nevertheless, before that we would like to note that the nucleon EM FFs $G_E^p(t)$, $G_M^p(t)$, $G_E^n(t)$, and $G_M^n(t)$ are very suitable for extraction of experimental information on the nucleon EM structure from the earlier mentioned physical quantities (3)–(9). For a construction of various nucleon EM structure models the flavor-independent isoscalar and isovector parts $F_{1s}^N(t)$, $F_{1v}^N(t)$, $F_{2s}^N(t)$, and $F_{2v}^N(t)$ of the Dirac and Pauli FFs to be defined by a parametrization of the matrix element

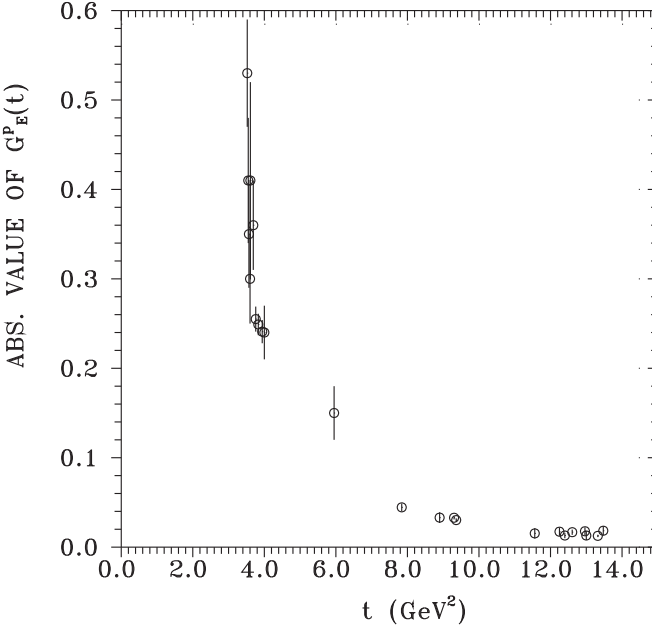


FIG. 3. Proton electric FF data in the timelike ($t > 0$) region from experiments in which $|G_E^p(t)| = |G_M^p(t)|$ has been assumed.

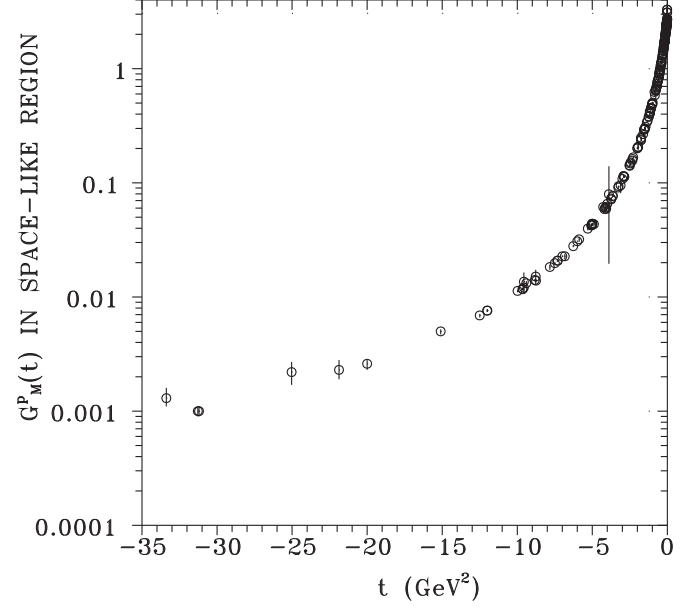


FIG. 4. Proton magnetic FF data in the spacelike ($t < 0$) region [16–23].

of the nucleon EM current

$$\begin{aligned} \langle N | J_\mu^{EM} | N \rangle \\ = e \bar{u}(p') \left\{ \gamma_\mu F_1^N(t) + \frac{i}{2m_N} \sigma_{\mu\nu} (p' - p)_\nu F_2^N(t) \right\} u(p) \end{aligned} \quad (13)$$

are more suitable.

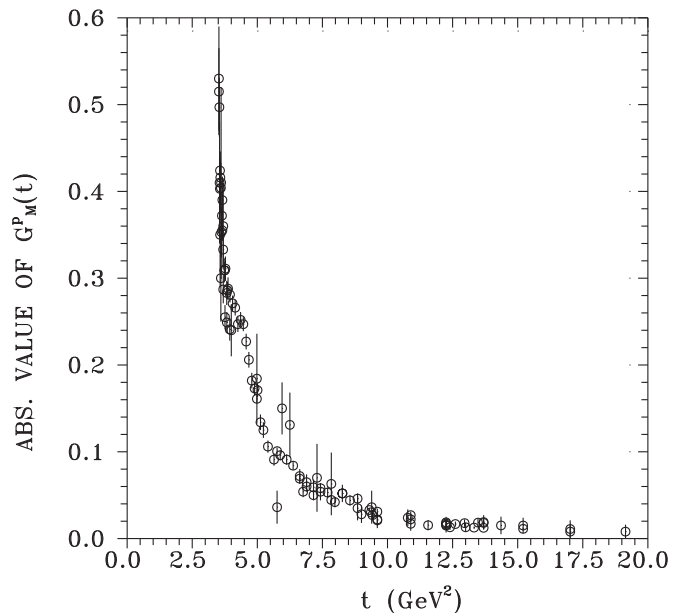


FIG. 5. Proton magnetic FF data in the timelike ($t > 0$) region [1,2,24–32].

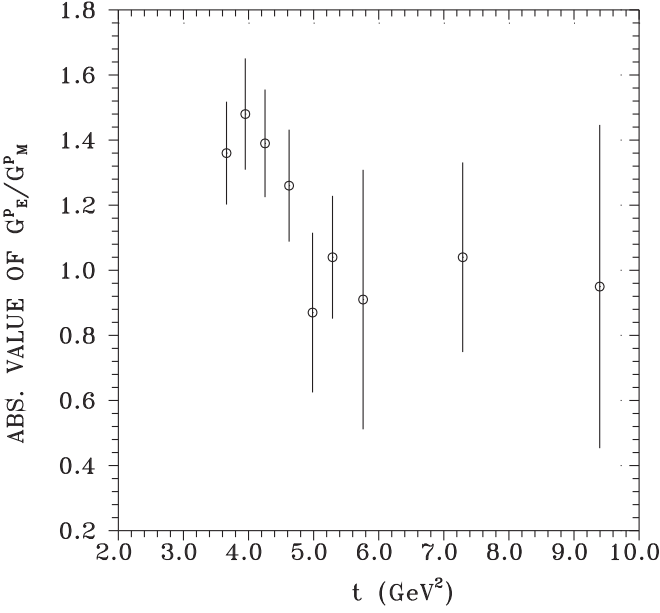


FIG. 6. Data on the ratio $|G_E^p(t)/G_M^p(t)|$ in the timelike ($t > 0$) region [1,2].

Both sets of these FFs are related as follows:

$$\begin{aligned} G_E^p(t) &= [F_{1s}^N(t) + F_{1v}^N(t)] + \frac{t}{4m_p^2} [F_{2s}^N(t) + F_{2v}^N(t)], \\ G_M^p(t) &= [F_{1s}^N(t) + F_{1v}^N(t)] + [F_{2s}^N(t) + F_{2v}^N(t)], \\ G_E^n(t) &= [F_{1s}^N(t) - F_{1v}^N(t)] + \frac{t}{4m_n^2} [F_{2s}^N(t) - F_{2v}^N(t)], \\ G_M^n(t) &= [F_{1s}^N(t) - F_{1v}^N(t)] + [F_{2s}^N(t) - F_{2v}^N(t)], \end{aligned} \quad (14)$$

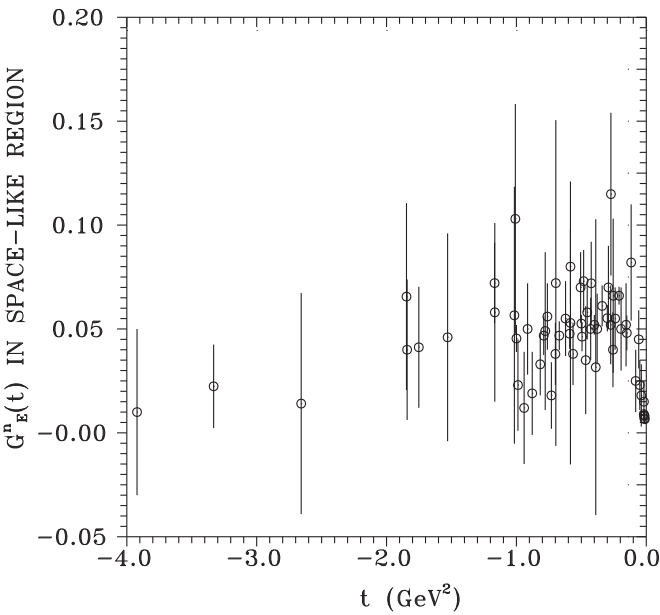


FIG. 7. Neutron electric FF data in the spacelike ($t < 0$) region [33–39].

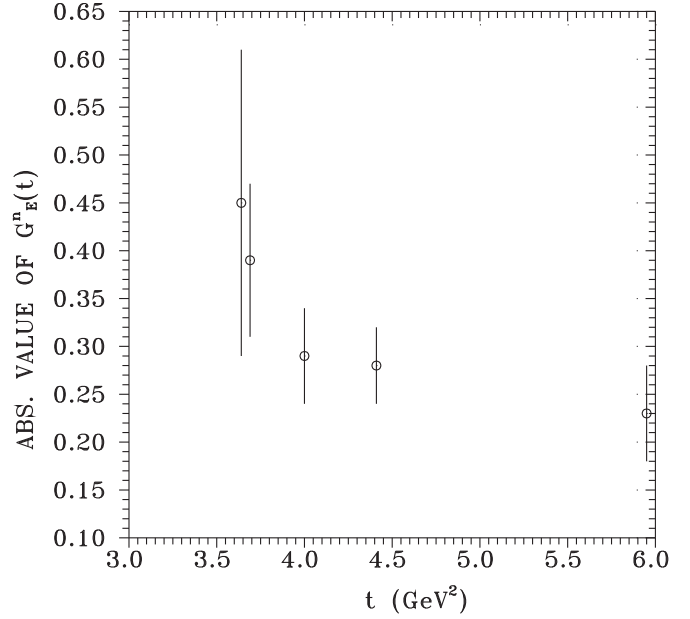


FIG. 8. Neutron electric FF data in the timelike ($t > 0$) region from experiments in which $|G_E^n(t)| = |G_M^n(t)|$ has been assumed.

whereby experimental fact of a production of true neutral vector-meson resonances with quantum numbers of the photon in $e^+e^- \rightarrow \text{hadrons}$ is in the first approximation taken into account by saturation of $F_{1s}^N(t)$ and $F_{2s}^N(t)$ with neutral isoscalar vector mesons $\omega(782), \phi(1020), \omega'(1420), \phi'(1680), \omega''(1650)$, and $\phi''(2170)$ [and $F_{1v}^N(t)$ and $F_{2v}^N(t)$] with neutral isovector vector-meson resonances $\rho(770), \rho'(1450)$, and $\rho''(1700)$ in the corresponding VMD FF parametrization in the zero-width approximation.

For the sake of generality let us consider FF $F(t)$ with a normalization $F(0) = F_0$, the asymptotic behavior

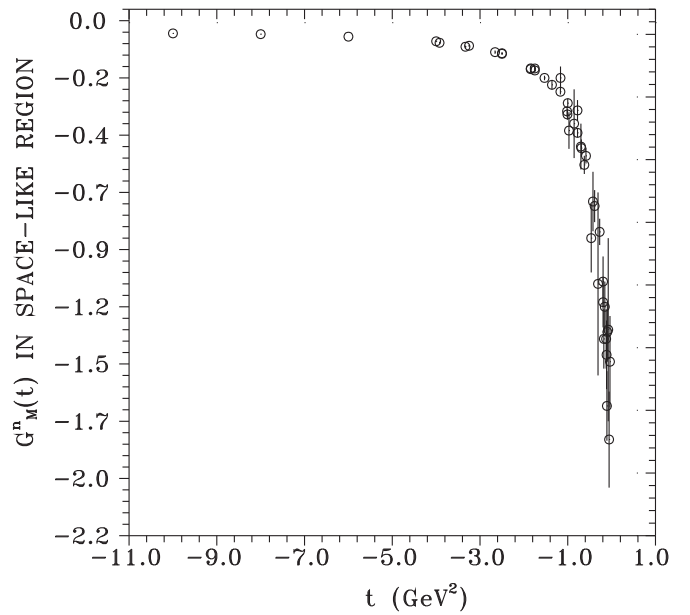


FIG. 9. Neutron magnetic negative FF data in the spacelike ($t < 0$) region [33,40–46].

TABLE I. The numerical values of the free parameters of the nucleon U&A EM structure model, respecting SU(3) symmetry, formulated in the previous section.

$t_{in}^{1s} = (1.0442 \pm 0.0200) \text{ GeV}^2$
$t_{in}^{2s} = (1.0460 \pm 0.1399) \text{ GeV}^2$
$t_{in}^{1v} = (2.9506 \pm 0.5326) \text{ GeV}^2$
$t_{in}^{2v} = (2.3449 \pm 0.7656) \text{ GeV}^2$
$(f_{\omega NN}^{(1)} / f_\omega) = (1.5717 \pm 0.0022)$
$(f_{\phi NN}^{(1)} / f_\phi) = (-1.1247 \pm 0.0011)$
$(f_{\omega' NN}^{(1)} / f_{\omega'}) = (0.0418 \pm 0.0065)$
$(f_{\phi' NN}^{(1)} / f_{\phi'}) = (0.1879 \pm 0.0010)$
$(f_{\omega NN}^{(2)} / f_\omega) = (-0.2096 \pm 0.0067)$
$(f_{\phi NN}^{(2)} / f_\phi) = (0.2657 \pm 0.0067)$
$(f_{\omega' NN}^{(2)} / f_{\omega'}) = (0.1781 \pm 0.0029)$
$(f_{\phi' NN}^{(2)} / f_{\phi'}) = (0.3747 \pm 0.0022)$

whereby the results are not very sensitive to the position of the effective inelastic thresholds t_{in}^{1s} , t_{in}^{2s} , t_{in}^{1v} , and t_{in}^{2v} .

The corresponding description of the data by means of this U&A model with numerical values of parameters given in Table I is shown in Figs. 12–19.

Of course one could not expect that a description of such gigantic set of data to be obtained from so many independent experiments, every one of them charged with corresponding statistical and systematical errors, will be consistent with rules of standard statistics. We have been able to reduce the total χ^2 on 522 deg of freedom only to the value 4.24.

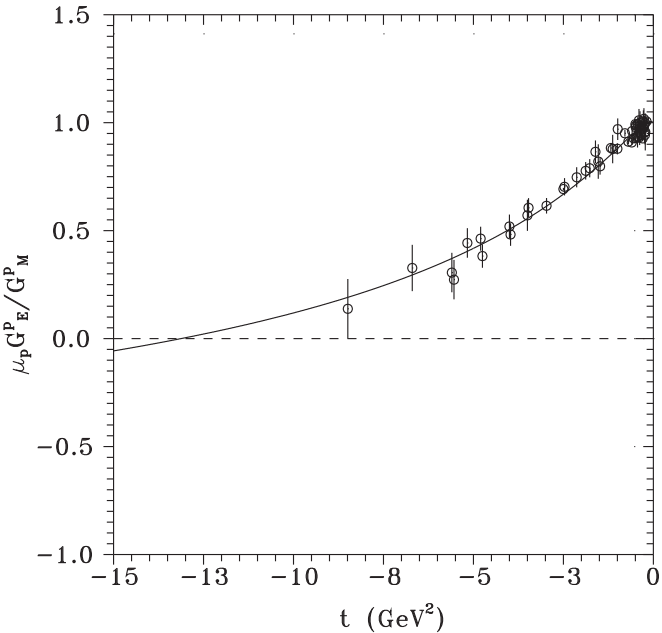


FIG. 12. Prediction of proton electric to magnetic FFs ratio behavior in spacelike region by U&A model respecting SU(3) symmetry and its comparison with existing data.

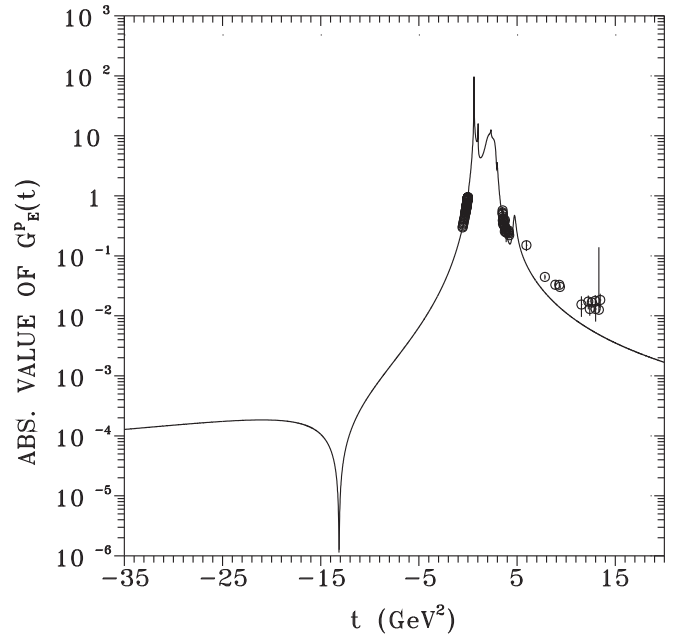


FIG. 13. Prediction of proton electric FF behavior by U&A model respecting SU(3) symmetry and its comparison with existing data.

The results of the analysis can be summarized as follows:

- (1) A reasonable description (see Fig. 12) of the most reliable nucleon EM structure data, i.e., the data on the ratio $\mu_p G_E^P(t) / G_M^P(t)$ in the spacelike region to be obtained in polarization experiments, is achieved.
- (2) Description of all other existing data (see Figs. 13–19) is quite reasonable too, besides an inconsistency of the data on neutron EM FFs in the timelike region with all

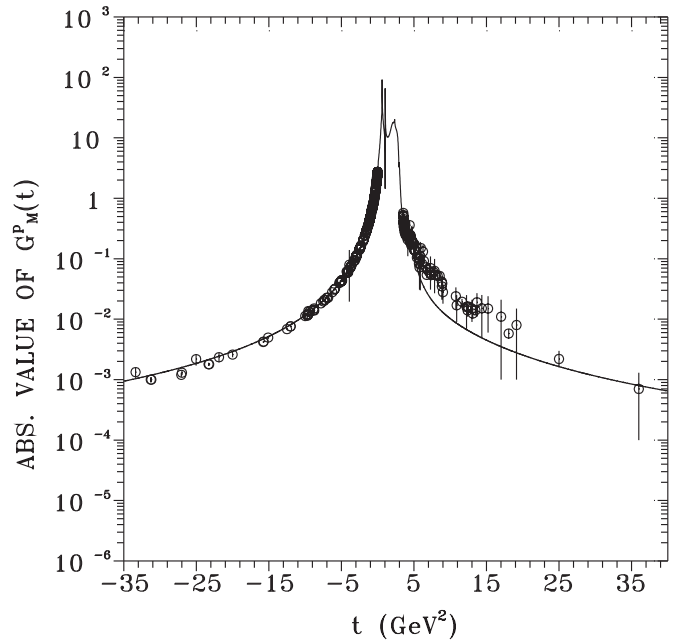


FIG. 14. Prediction of proton magnetic FF behavior by U&A model respecting SU(3) symmetry and its comparison with existing data.

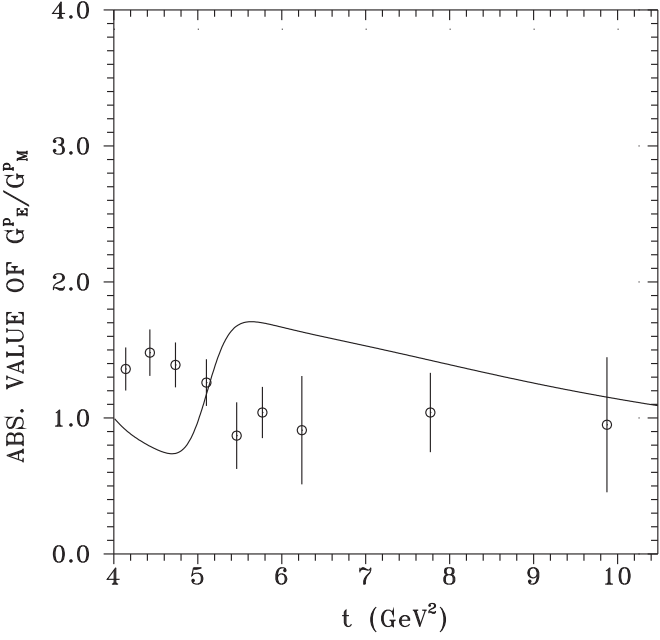


FIG. 15. Prediction of the absolute value of proton electric to magnetic FFs ratio behavior in the timelike region by the U&A model with respect to SU(3) symmetry and its comparison with existing data.

other data on nucleon EM FFs, indicating that the total cross section of $e^+e^- \rightarrow n\bar{n}$ is considerably larger than has been found in FENICE experiment [28]. So, we are coming to the same conclusions as pointed out by one of the authors in Refs. [50,51] published more than 25 years ago.

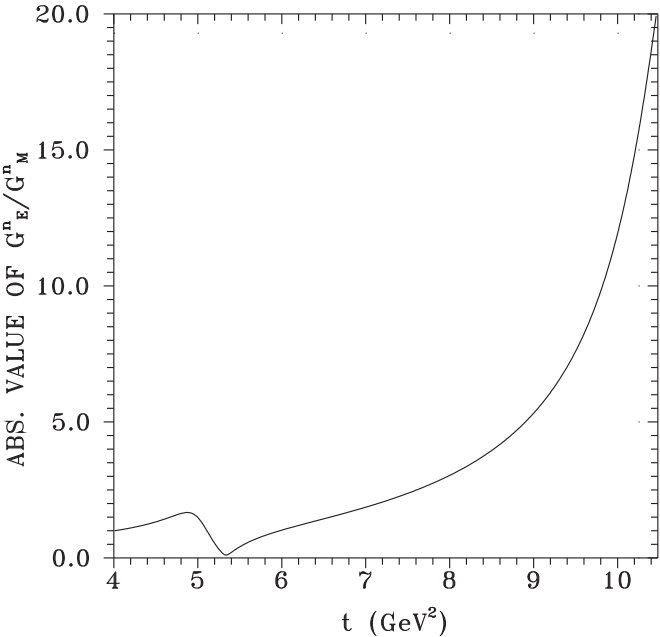


FIG. 16. Prediction of the absolute value of neutron electric to magnetic FFs ratio behavior in the timelike region by the U&A model with respect to SU(3) symmetry.

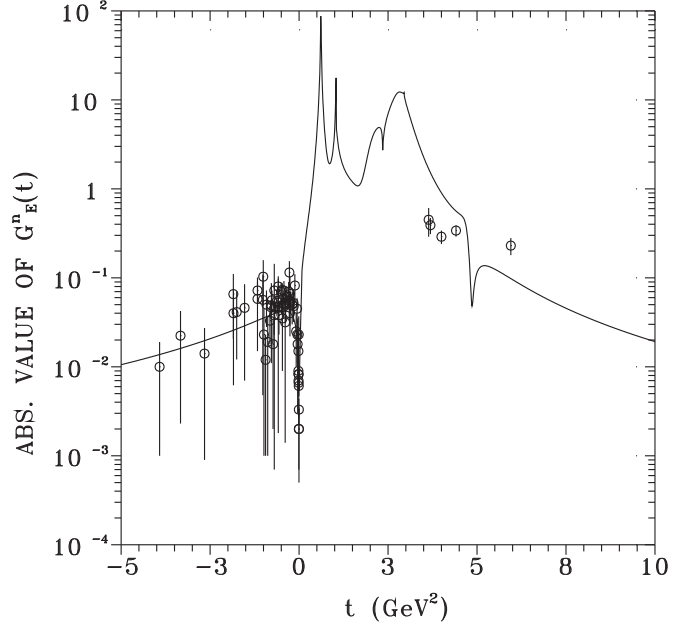


FIG. 17. Prediction of neutron electric FF behavior by the U&A model with respect to SU(3) symmetry and its comparison with existing data.

- (3) Again the existence of the zero of the proton electric FF $G_E^p(t)$ approximately at $t_z = -13$ GeV 2 is confirmed, which has been predicted in Ref. [52] for the first time.
- (4) Electric and magnetic mean square charge radii of the nucleons are determined to be $\langle r_{Ep}^2 \rangle = (0.7182 \pm 0.0369)$ fm 2 , $\langle r_{Mp}^2 \rangle = (0.7573 \pm 0.0133)$ fm 2 , $\langle r_{En}^2 \rangle = (-0.1162 \pm 0.0369)$ fm 2 ,

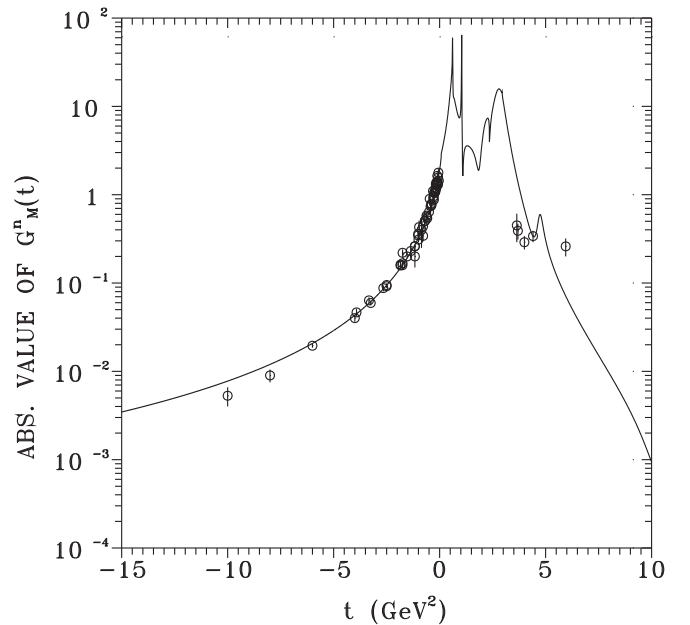


FIG. 18. Prediction of neutron magnetic FF behavior by the U&A model respecting SU(3) symmetry and its comparison with existing data.

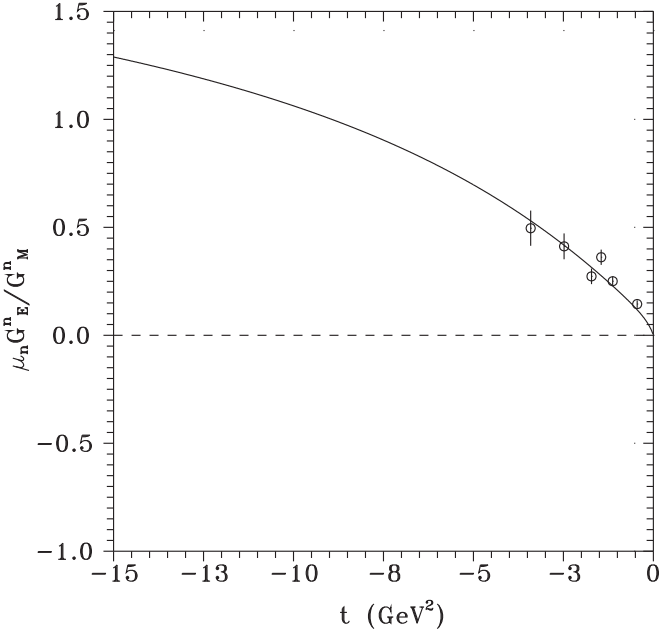


FIG. 19. Prediction of neutron electric to magnetic FFs ratio behavior in the spacelike region by the U&A model respecting SU(3) symmetry and its comparison with existing data.

$\langle r_{Mn}^2 \rangle = (0.8312 \pm 0.0195) \text{ fm}^2$. Since the electric root mean square charge radius of the proton has been obtained by the U&A model simultaneously describing all existing 11 data sets on nucleon EM structure and its value is consistent with the value $\langle r_{Ep} \rangle = 0.84184 \pm 0.00067 \text{ fm}$ determined in the muon hydrogen atom spectroscopy [53], it seems to us that the electric proton charge radius puzzle is solved. Recently, researchers [54] also analyzing the nucleon EM structure data using by another approach came to the same conclusions..

- (5) Electric mean square charge radius of the neutron is found to be almost identical with the value given in Ref. [8].

In Figs. 20–25 it is clearly demonstrated that the nucleon EM FFs represented by the U&A model indeed fulfill the reality condition $G^*(t) = G(t^*)$, i.e., they all are real functions from $-\infty$ up to the lowest branch point $t_0 = 4m_\pi^2$ on the positive real axis.

The imaginary parts of all nucleon EM FFs are different from zero only from the lowest branch point at $t = 0.0784 \text{ GeV}^2$ to $+\infty$ and their behaviors are given by the unitarity conditions of the corresponding FFs.

V. NUMERICAL VALUES OF THE f^F, f^D, f^S AND $f^{F'}, f^{D'}, f^{S'}$ COUPLING CONSTANTS

The SU(3) invariant Lagrangian (2) of vector-meson nonet $\rho^-, \rho^0, \rho^+, K^{*-}, K^{*0}, \bar{K}^{*0}, K^{*+}$, and ω, ϕ with $1/2^+$ octet baryons $p, n, \Lambda, \Sigma^+, \Sigma^0, \Sigma^-, \Xi^0$, and Ξ^- provides the

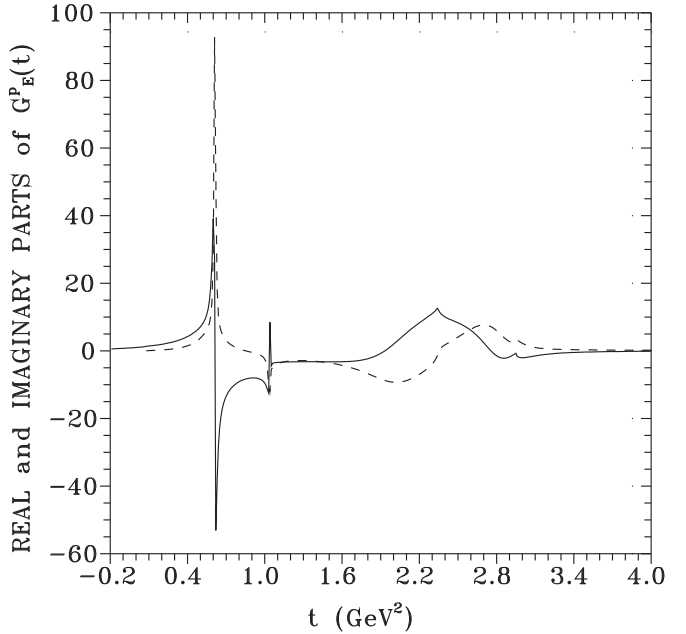


FIG. 20. Prediction of real (solid line) and imaginary (dashed line) parts of the proton electric FF by the U&A model respecting SU(3) symmetry.

following expressions:

$$\begin{aligned} f_{\rho NN}^{(1)} &= \frac{1}{2}(f_1^D + f_1^F), \\ f_{\omega NN}^{(1)} &= \frac{1}{\sqrt{2}}f_1^S \cos \theta - \frac{1}{2\sqrt{3}}(3f_1^F - f_1^D) \sin \theta, \\ f_{\phi NN}^{(1)} &= \frac{1}{\sqrt{2}}f_1^S \sin \theta + \frac{1}{2\sqrt{3}}(3f_1^F - f_1^D) \cos \theta, \end{aligned} \quad (51)$$

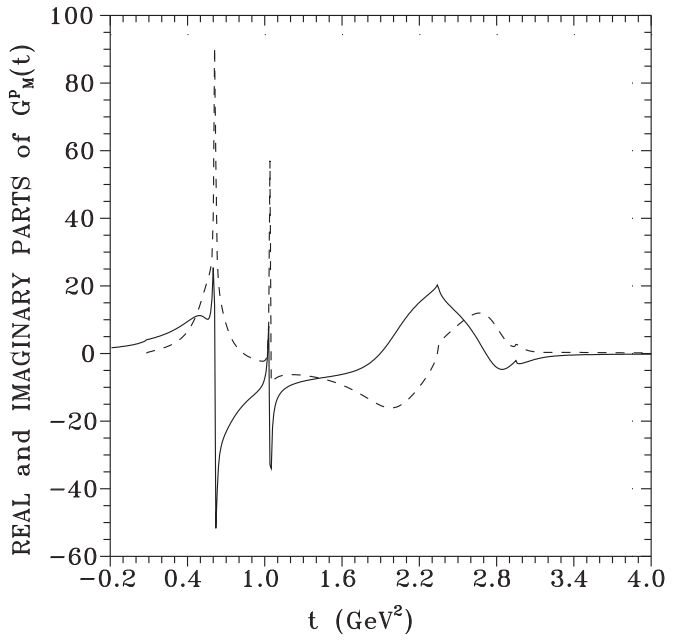


FIG. 21. Prediction of real (solid line) and imaginary (dashed line) parts of the proton magnetic FF by the U&A model respecting SU(3) symmetry.

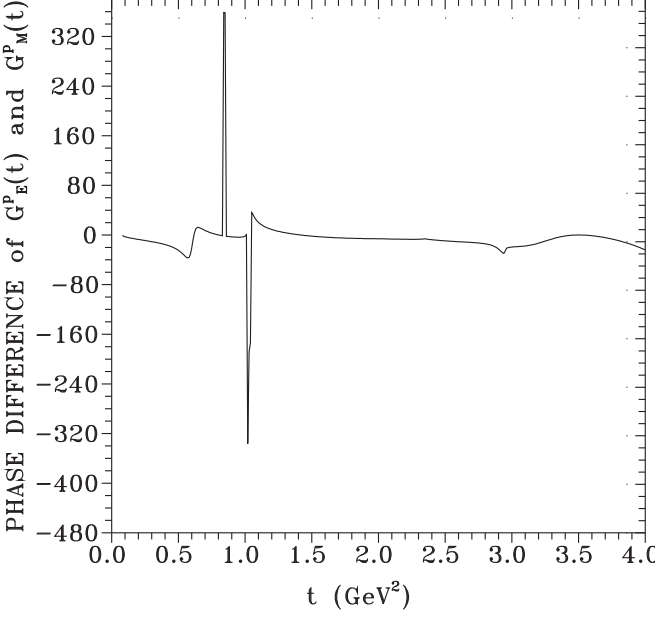


FIG. 22. Prediction of a phase difference of the proton electric and magnetic FFs by the U&A model with respect to SU(3) symmetry.

and

$$\begin{aligned} f_{\rho NN}^{(2)} &= \frac{1}{2}(f_2^D + f_2^F), \\ f_{\omega NN}^{(2)} &= \frac{1}{\sqrt{2}}f_2^S \cos \theta - \frac{1}{2\sqrt{3}}(3f_2^F - f_2^D) \sin \theta, \quad (52) \\ f_{\phi NN}^{(2)} &= \frac{1}{\sqrt{2}}f_2^S \sin \theta + \frac{1}{2\sqrt{3}}(3f_2^F - f_2^D) \cos \theta, \end{aligned}$$

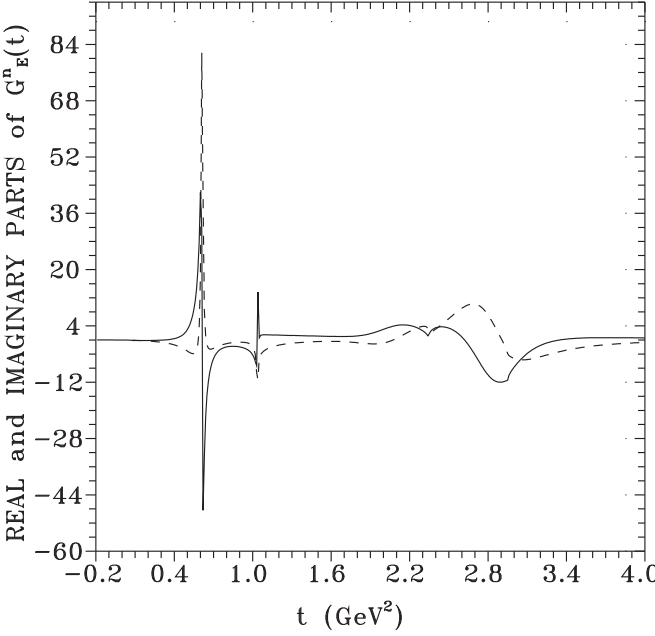


FIG. 23. Prediction of real (solid line) and imaginary (dashed line) parts of the neutron electric FF by the U&A model with respect to SU(3) symmetry.

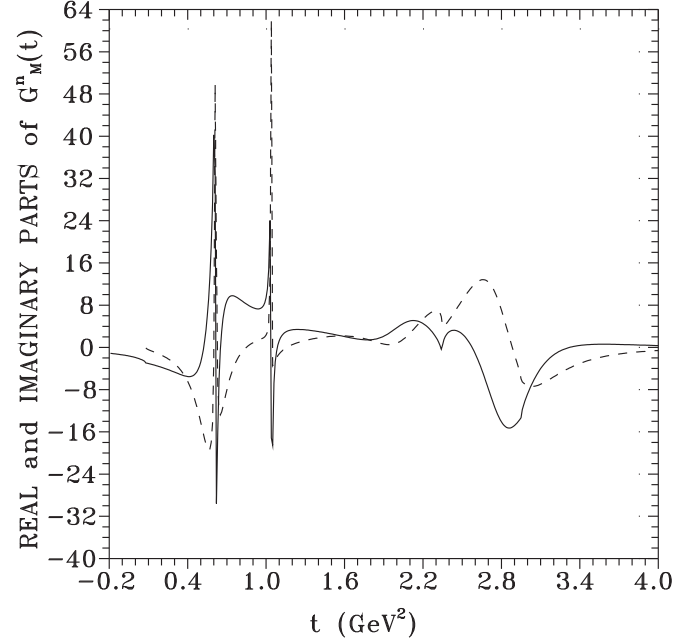


FIG. 24. Prediction of real (solid line) and imaginary (dashed line) parts of the neutron magnetic FF by the U&A model with respect to SU(3) symmetry.

where angle $\theta = 43.8^\circ$ and it is given by the Gell-Mann-Okubo quadratic mass formula:

$$m_{\phi(1020)}^2 \cos^2 \theta + m_{\omega(782)}^2 \sin^2 \theta = \frac{4m_{K^*(892)}^2 - m_{\rho(770)}^2}{3}. \quad (53)$$

From the SU(3) invariant Lagrangian of the first excited vector-meson nonet $\rho^-, \rho^0, \rho^+, K^{*-}, K^{*0}, \bar{K}^{*0}, K^{*+}, \omega$, and ϕ' with $1/2^+$ octet baryons $p, n, \Lambda, \Sigma^+, \Sigma^0$,

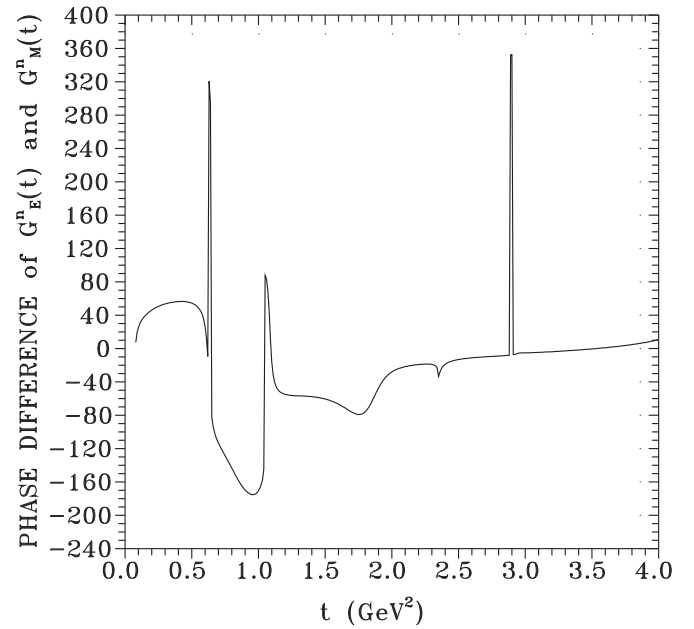


FIG. 25. Prediction of a phase difference of the neutron electric and magnetic FFs by the U&A model with respect to SU(3) symmetry.

- [35] S. Galster *et al.*, Nucl. Phys. B **32**, 221 (1971).
- [36] W. Bartel *et al.*, Phys. Lett. B **39**, 407 (1972).
- [37] D. I. Glazier *et al.*, Eur. Phys. J. A **24**, 101 (2005).
- [38] G. Warren *et al.*, Phys. Rev. Lett. **92**, 042301 (2004).
- [39] J. Golak *et al.*, Phys. Rev. C **63**, 034006 (2001).
- [40] S. Rock *et al.*, Phys. Rev. Lett. **49**, 1139 (1982).
- [41] H. Anklin *et al.*, Phys. Lett. B **428**, 248 (1998).
- [42] G. Kubon *et al.*, Phys. Lett. B **524**, 26 (2002).
- [43] P. Markowitz *et al.*, Phys. Rev. C **48**, R5 (1993).
- [44] A. Lung *et al.*, Phys. Rev. Lett. **70**, 718 (1993).
- [45] E. E. W. Bruins *et al.*, Phys. Rev. Lett. **75**, 21 (1995).
- [46] B. Anderson *et al.*, Phys. Rev. C **75**, 034003 (2007).
- [47] B. Plaster *et al.*, Phys. Rev. C **73**, 025205 (2006).
- [48] S. Riordan *et al.*, Phys. Rev. Lett. **105**, 262302 (2010).
- [49] S. Dubnička, A. Z. Dubničková, and P. Weisenpacher, Eur. Phys. J. C **32**, 381 (2004).
- [50] S. Dubnička, Nuovo Cim. **100**, 1 (1988).
- [51] S. Dubnička, Nuovo Cim. **103**, 1417 (1990).
- [52] C. Adamuscin, S. Dubnička, A. Z. Dubničková, and P. Weisenpacher, Prog. Part. Nucl. Phys. **55**, 228 (2005).
- [53] R. Pohl *et al.*, Nature (London) **466**, 213 (2010).
- [54] U.-G. Meissner *et al.*, Eur. Phys. J. A **48**, 151 (2012).
- [55] A. Bramon, *Lecture on Electromagnetic Interactions of Hadrons*, UAB-FT-D-3 (Bellaterra Universitat Autònoma Barcelona, 1979).